

New insights on blue pigments used in 15th Century paintings by Synchrotron Radiation micro FTIR and XRD

Nati Salvadó¹, Salvador Butí¹, Miguel A. G. Aranda², Trinitat Pradell³

1. Dpt. d'Enginyeria Química. EPSEVG. Universitat Politècnica de Catalunya, Av. Víctor Balaguer s/n, 08800 Vilanova i la Geltrú, Barcelona

2. ALBA-CELLS synchrotron, Carretera BP 1413, Km. 3.3, E-08290 Cerdanyola, Barcelona, Spain

3. Dpt. Física i Enginyeria Nuclear. ESAB. Universitat Politècnica de Catalunya, Campus del Baix Llobregat. Av. del Canal Olímpic 15, 08860 Castelldefels, Barcelona

* Corresponding author:

E-mail address: nativitat.salvado@upc.edu

Telephone: 0034938967717

Fax: 0034938967700

Keywords: blue pigments, lapis lazuli, azurite, indigo, cultural heritage, synchrotron radiation, FTIR, XRD

ABSTRACT

The blue pigments used on altarpieces in 15th Century in Catalonia and Crown of Aragon are principally the azurite mineral. To a lesser extent lapis lazuli, also of mineral origin and occasionally, in the background areas, outlining the figures, and for the chromatic ground layer, indigo, were used. Data from several altarpieces belonging to well-known artists of the time is presented. Synchrotron radiation X-ray diffraction (SR-XRD), micro-infrared spectroscopy (μ -FTIR), synchrotron radiation micro-infrared spectroscopy (μ SR-FTIR), Raman spectroscopy, scanning electron microscopy with X-ray microanalysis (SEM-EDS) are used. X-ray diffraction and infrared spectroscopy in association with synchrotron radiation have shown to be especially interesting due to the micron spot sizes, high brilliance and energy tunability which help to obtain good separation of the signals coming from different phases/substances and their localization in the various paint layers. Examples are presented which illustrate the potential of each analytical technique for the identification of this kind of materials in the 15th century paintings. The natural origin and composition of the pigments and its distribution in the paint layers are determined and some correlations with other contemporary paintings obtained. Finally, the alteration compounds related to blue pigments are determined in each case.

INTRODUCTION

The study of ancient paintings, and in particular Gothic altarpieces, is a challenge for the analytical chemists owing to the small size of the samples, the micrometric layered paint structure (typical layer thicknesses vary between 10 and 100 μ m), the high number (5 or more) of different substances, low amount (in some cases a few particles dispersed in the layer) and diverse nature of the compounds (pigments, binders, impurities and aging and reaction compounds). Consequently, there is not an optimal single analytical technique valid for the determination of all the compounds. Additionally, the determination of the spatial distribution and morphology of the compounds is, often, as important as the chemistry and speciation of the pigment particles.

Different levels of sensitivity are required to determine the main inorganic and organic fractions and impurities present. The identification of the impurities provides information not only about the pigment source and/or synthesis, but also about the reaction and aging compounds present, which is essential for verifying the reactivity and stability of the paint layers.

As a consequence, a variety of analytical techniques are being used in the study of ancient paintings, i.e. separation techniques, X-ray fluorescence (XRF), Scanning Electron Microscope with an Energy Dispersive Spectrometer (SEM-EDS), Raman Spectroscopy, Fourier Transform Infrared Spectroscopy (FTIR), X-ray diffraction (XRD), etc.¹⁻⁶

This paper illustrates how specific sample preparation and a tailored-combination of analytical techniques can solve most of the analytical problems encountered in the study of the blue paints in altarpieces from the 15th century. Information is obtained with regard to the painting techniques and the materials present, including pigments, binders, reaction compounds, impurities and reagents remaining in the original pigments, as well as on their morphology and spatial distribution.

The usefulness of synchrotron radiation (SR) in the characterization of materials in ancient paintings has already been demonstrated in a number of studies⁷⁻⁹. SR allows focusing on areas as small as a few micrometers, obtaining spectra of very high signal to noise ratio thanks to the high brilliance, collimation and monochromaticity of the beam. The combination of FTIR and XRD is particularly useful for the study of ancient paint layers.

A typical 12-15 μm spot size may be used with mid $\mu\text{SR-FTIR}$ ($650\text{-}4000\text{cm}^{-1}$); the small spot and a specific sample preparation (pressing small fragments extracted from each layer in a diamond cell) permits the separation and identification of compounds even when present in minor amounts. The high selectiveness of the small spot analyzed compensates the relatively low detection limit of FTIR. Commercially available FTIR microscopes are only fitted with mid-IR detectors. However, many substances of interest such as oxides, sulphides, chlorides show IR absorption bands below 700cm^{-1} . Other substances show their absorption bands overlapping with those from other compounds in the mid-infrared region but not in the far-infrared region. The far infrared region ($700\text{-}200\text{cm}^{-1}$) can be reached by including a bolometer. However, in this region, diffraction limits the lowest spot size to about $50\ \mu\text{m}$.

SR-XRD in transmission geometry with square or rectangular spot sizes as small as, $20\ \mu\text{m}$ by $50\ \mu\text{m}$, is optimal for the study of the layered structure of the paint layers. Cross sections of the paint samples are prepared with typical thicknesses that vary, depending on the stability of the material, between $100\ \mu\text{m}$ and $200\ \mu\text{m}$ for the Gothic paintings under study. The small spot has a high selectiveness, and although the sensitivity of XRD is not very high (between 1-5% depending on peak overlapping and crystallinity of the substance) the use of a small spot reduces the detection limit to low values.

High resolution SR-XRD, by means of multi crystal analyzer detector system working in transmission geometry, is chiefly characterized by its high angular resolution. High angular resolution is very important to separate overlapping XRD diffraction peaks, usually happening in the paint layers due to the large number of contributing phases. A wide angular range is fundamental for the quantification of the various compounds present by Rietveld refinement of the data. In this case, we do not have the same high

focusing capability, but the high angular resolution and large angular range reached can reduce detection limits down to 0.1 wt% for the compounds determined herewith.

A combination of mid and far μ SR-FTIR, μ SR-XRD and high resolution SR-XRD is able to identify most of the compounds of interest. These tools plus SEM-EDS, which provides elemental composition, spatial distribution and morphology of the particles in the paint layers, is used in the present study for the investigation of the blue paints in the altarpieces. Raman spectroscopy has also been used to complement some of the analysis. The examples presented herewith illustrate the potential of each analytical technique for the analysis of this type of materials.

The present study focuses on the altarpiece paintings produced in Catalonia and the Crown of Aragon during the 15th century. The blue samples belong to a set of artworks selected to include both tempera and oil techniques and the different schools from the territory. Following these criteria the following altarpieces have been selected: “Saint John and Saint Stephen” (1455-1453) by Honorat Borrassà[†] and “The Virgin” by Joan Antigó, painted with oil and egg tempera respectively both from the Girona School; “Constable” (1465) by Jaume Huguet and “Saint Vincent” (1455-1460) by Bernat Martorell belonging to the school of Barcelona both painted mainly with egg tempera and the altarpiece “Our Lady of the Counsellors” by Lluís Dalmau from Barcelona painted with oil; “The Virgin” by Pasqual Ortoneda (1459) from the school of Tarragona painted with a glue tempera technique; “The apparition of the Virgin to Saint Francis in the Porciuncula” from the Valencian school painted in a mixed technique. This last altarpiece and those by Honorat Borrassà and Bernat Martorell are on display at the MNAC (Museu Nacional d’Art de Catalunya) in Barcelona¹⁰; Jaume Huguet’s is displayed, in its original location, the chapel of “Santa Àgata” in the Royal Palace in Barcelona; Pasqual Ortoneda’s is displayed in the VINSEUM museum, in Vilafranca del Penedès, Barcelona. Finally, the altarpiece by Joan Antigó is displayed in its original location in the monastery of Saint Stephen in Banyoles, Girona.

Taking into account the analysis carried out and the documents studied, the blue pigment used in this period and geographical area is mainly the mineral azurite, to a lesser extent lapis lazuli, also of mineral origin and occasionally, indigo of vegetal origin which was applied in the background areas, outlining the principal figures, and/or for the chromatic preparation layer.

All the data presented in this paper have been compiled from the analysis performed during several years study.

SAMPLE PREPARATION AND ANALYTICAL METHODS

Optical Microscopy (OM) and Scanning Electron Microscopy (SEM), JEOL-5600, with elemental analysis (PCXA LINK EDS) are used in order to obtain information of the composition, size distribution and homogeneity of the particles in the paint samples. Small fragments or cross sections were carbon coated to ensure good electrical conductivity necessary to perform the SEM-EDS analysis (20kV or 25 kV of voltage and 1 nA of current). In order to obtain the cross sections, small fragments were embedded in a polyester resin polymerized by a peroxo organic catalyser in conditions of low humidity. After polymerization, a cut was made with a precision low speed saw

[†] Currently the MNAC attributes this work to the master of Sant Joan i Sant Esteve.

with a diamond wafering blade (150 micron thickness), which allows precise cutting, and it was thinly polished with 1 μ m size diamond paste. Water was the only fluid used for lubrication and was kept to the minimum possible to avoid sample damaging. For sample embedding a polyester resin was chosen because it shows, considering the characteristic of the samples, the most adequate set of properties: the temperature does not increase during polymerization and has adequate hardness for cutting and polishing, polishing time is minimised avoiding water. Thin cuts, 100 to 200 μ m thick, are also performed by shifting the diamond blade, these thin cuts were used to perform transmission μ SR-XRD measurements.

Synchrotron based micro X-ray diffraction (μ SR-XRD) data were obtained at beamline BM16 of the European Synchrotron Radiation Facility (ESRF, Grenoble). Small fragments cut from the samples were previously selected with the help of the optical microscope. These fragments were placed on an adhesive support from where measurements were taken in transmission geometry using a beam footprint of 30 \times 30 microns. Thin cross sections were also prepared from some selected samples –150 microns thick. A beam footprint of about 20 \times 50 μ m² was found to be the most adequate for the discrimination of the compounds present in the different layers. A smaller beam footprint may lead to a spotty single crystal-like 2D X-ray diffraction pattern, dominated by only some of the big crystallites precluding the identification of the other compounds. A larger footprint, hampers separation of the compounds present in the different layers. The setup included a CCD ADSC Q210r detector and 10keV (λ =1.24 \AA) or 12.7keV (λ =0.98 \AA) X-rays. This setup provides high sensitivity to compounds present in very low amounts and a low angular limit adequate for some of the organic compounds present but has some limitations in the angular resolution for highly overlapping diffraction patterns.

High angular resolution SR-XRD measurements were also performed at beamline BM01 (ESRF). For these measurements, small fragments of the sample were placed in a glass capillary to allow spinning which improve the particle statistics. A two circle diffractometer with three line detectors measuring an angle of 5 $^\circ$ was used. Measurements were taken in Debye-Scherrer transmission geometry at 24.9 keV (0.50 \AA). A 2 θ range of 25 $^\circ$ was recorded for a period of 15 hours. After measurements, the paint fragments can be taken out of the glass capillary and prepared for and used with other analytical techniques.

Synchrotron-based micro infrared spectroscopy (μ SR-FTIR) 4000-650 cm^{-1} range measurements were taken at various beamlines; MIRIAM beamline of the Diamond Light Source setup consists on a Bruker 80 V Fourier Transform IR Interferometer coupled with a Hyperion 3000 microscope, with a 100 \times 100 micron area broad band, and MCT detector. SMIS beamline at Soleil Synchrotron setup includes a Thermo Nicolet Continuum XL FT-IR imaging microscope with MCT detector. Far μ SR-FTIR range measurements were performed at IR 1 beamline of ANKA synchrotron light source, Forschungszentrum Karlsruhe, Germany. The Bruker IFS 66v/s spectrometer was equipped with a Bruker IRScope II microscope a bolometer for the far-infrared working at 4.2K for the 700-200 cm^{-1} interval. In all cases, in order to perform transmission measurements flat samples of adequate thickness (about 2 μ m thick) were obtained by squeezing them between the two diamond windows of an anvil cell fragments previously cut and selected under the optical microscope. The spectra were obtained through only one of the windows. Spectra were obtained in transmission mode and from different areas using a microbeam of either 12 \times 12 microns or 15 \times 15 microns

for mid-FTIR and 50×50 microns for far-FTIR at the sample defined by the slits. For each measurement, 128 scans were recorded with a resolution of 4 cm⁻¹.

Raman Spectra recorded using a Thermo Scientific DXR Raman microscope, 633 nm excitation, 100x objective lens, with ≤1 mW power. This equipment is available at SMIS beamline of Soleil synchrotron).

RESULTS AND DISCUSSION

Lapis lazuli

Lluís Dalmau used *lapis lazuli* in the blue paint layers in the altarpiece “The Virgin of the Counsellors”¹¹. *Lapis lazuli* is a semiprecious stone and was an expensive pigment scarcely used in 15th century paintings from the Crown of Aragon. Its presence must be associated to the importance of an artwork that was going to be exhibited at the front of the Chapel of the City Hall. In fact, Lluís Dalmau was required to use *blau d’Acre (lapis lazuli)* in the terms of the contract dated October 29th, 1443. Fig. 1a,b shows the sample extracted from the cloak of one of the choir angels. The paint is formed by a sequence of layers containing particles of increasing particle size from the surface to the ground. The first two layers (25 μm and 65 μm thick, respectively) contain *lapis lazuli* particles and drying oil; the third layer contains coarser *lapis lazuli* particles mixed with some particles of lead white, drying oil and lead carboxylates. Below, a fourth layer (50 μm thick) containing coarse angular azurite -Cu₃(CO₃)₂(OH)₂- particles, lead white, drying oil and some lead carboxylates. The sequence of *lapis lazuli*/azurite layers and the increasing particle size is the same described for the blue clothes in the “Adoration of the Mystic Lamb” (exhibited in the Cathedral of Gent, Belgium) from Jan Van Eyck¹², a Flemish panel painting with which “Our Lady of the Counsellors” shares clear stylistic similarities. According to historical documents Dalmau lived about five years in Flanders supported by the King Alfons el Magnànim, to learn about the Flemish ARS NOVA¹¹. The data obtained herewith provides for the first time evidence of the direct link existing between Lluís Dalmau and Van Eyck’s workshop.

μSR-XRD analysis of different areas of the *lapis lazuli* layers show the presence of lazurite-(Na,Ca)₄₋₈[Al₆Si₆O₂₄](SO₄,S)₁₋₂-, nepheline -Na₃(Na,K)[Al₄Si₄O₁₆]-, sodalite -Na₈[Al₆Si₆O₂₄]Cl₂-, quartz -SiO₂-, sanidine/albite -(Na,K)(Si₃Al)O₈- and, in some spots phlogopite -K₂(MgFe)₆[Si₆Al₂O₂₀](OH)₄- is also detected, see Fig. 1c. Lazurite and sodalite are the minerals responsible for the blue colour while the other minerals are associated with the original deposits. A high resolution SR-XRD powder pattern was obtained from one of the fragments. This pattern was analysed by the Rietveld method to obtain the quantitative phase analysis. The fitting is very good as shown in Fig. 2 (difference curve is very flat). The output of the analysis is given in Table 1. The whole blue painting layer contains 24.6 wt% of azurite and 75.4% of minerals related to the *lapis lazuli* (see Table 1). From this analysis, it is possible to retrieve the mineral content of the *lapis lazuli* layer which contains 62.4% lazurite, 23.6% nepheline, 6.9% quartz, 6.1% sodalite and 1.0% sanidine, by renormalization to 100 wt%. Other minerals if present must be in amounts below 0.1%. Unit cell values are also reported in Table 1 as their values could give insight about the *lapis lazuli* provenance by comparison with data to be reported in other studies. Some of the reported phases were also identified by FTIR and the data are shown in Fig. 3. The occurrence of associated minerals indicates the natural origin of the *lapis lazuli*; artificial *ultramarine* has a composition similar to lazurite with uniform, small and round particles¹³. Moreover, the

presence of an infrared sharp band at 2340 cm^{-1} and small satellite peak at 2274 cm^{-1} (asymmetric stretching ν_3 of $^{12}\text{CO}_2$ and $^{13}\text{CO}_2$ respectively) is related to CO_2 adsorbed into the structure of sodalite and also confirms the natural origin of the *lapis lazuli*¹⁴⁻¹⁶ (Fig. 3b). The band at 2040 cm^{-1} might be assigned to $\nu(\text{CO})$ (adsorbed carbon monoxide) and may be linked to the purification process followed¹⁷. The amount of sodalite (sodalite/lazurite ratio=10%) compares very well to the *lapis lazuli* used by Michelangelo in the fresco of the Last Judgment (12%)¹⁸ and could indicate the same geographical origin¹³. However, the relatively higher amounts of nepheline and quartz (nepheline/lazurite ratio=38%, quartz/lazurite ratio=7%) than in the pigment used by Michelangelo (17% and 4% respectively) may also indicate the use of a less pure pigment. Purification methods for removing the greyish particles from the blue pigment are described in contemporary paint treatises^{17,19}.

Small particles of lead white ($1\ \mu\text{m}$) present in both, the azurite and *lapis lazuli* layers must have been added to benefit from the oil drying capability of the lead white. The formation of lead carboxylate salts from the reaction of the free fatty acids present in the oil with the lead white is known to trigger the drying process. The amount of lead white particles present is very low, actually lower than 0.1% otherwise the Rietveld refinement would have determined them.

Finally, Lluís Dalmau mixed the *lapis lazuli* with drying oil, which is not most adequate considering that the refraction index of both *lapis lazuli* and oil are similar (about 1.5) and consequently, the scattered light is low and, accordingly is the opacity.

Azurite

Azurite is a mineral pigment²⁰ that was widely used in 15th century wood paintings from the Crown of Aragon. Relevant areas of the altarpieces were painted with this pigment as for instance the mantel of the Virgins. Currently, these areas appear almost black or very dark.

Fig. 4a,b OM and SEM images corresponding from a cross section of a sample taken from the mantel of the virgin in “Constable” altarpiece. The azurite particles can be seen and the environmental superficial layer deposition, perfectly integrated into the paint layer.

The causes for this darkening can be found in the large particle size, between 2 and 30 μm , of the pigment that was used. These particle sizes were necessary to obtain saturated colours as smaller sizes produce less saturated blues. The use of large particles creates larger interstitial gaps between them which are often not totally filled by the binding media. However, the amount of binding media is greater than that found in those painting layers obtained with lower particle size pigments also increasing the darkening. The darkening of the binding media is due to the aging of the organic compounds, in the case shown in Fig. 4, the proteins from the animal glue. The fact that the darkening is more evident towards the surface (Fig. 4a) suggests that this is not the sole cause of the colour alteration. The fact that the particle sizes at the surface are more irregular, favours the retention of dust and pollution deposited from the environment such as, carbon –from the candles and oil lamps used in the lighting-, gypsum, oxalates and silicates; they become integrated in the pictorial layers and even, in some cases, consolidated as a consequence of the subsequent application of varnish layers. This makes the restoration of the original blue hues unviable. The elimination of the upper

layers would cause the necessary loss of the pigment and as a consequence the nuances and motifs of the clothing.

Fig. 4b, shows the presence of a white contrasted particle composed of S and Ba. These particles can be detected using backscattering electrons as they have a larger average atomic weight than the surrounding particles and organic matrix (Fig. 1b, 4b). The sporadic presence of these particles is commonly observed in samples containing azurite of mineral origin. They are barium sulphate, a material of paragenesis (mineral association) with azurite. This is one further indicator of the mineral origin of the pigment.

It is also worth to notice from the analysis of several samples from altarpieces of this period that small amounts of malachite $\text{CuCO}_3 \cdot \text{Cu}(\text{OH})_2$ are often identified. Malachite could be one of the natural impurities present in the original mineral or a weathering product of azurite. This last hypothesis is the most probable considering that we have been able to determine the presence of intermediate compounds between the structure of azurite and those of malachite. This can be seen in sequence of $\mu\text{SR-FTIR}$ spectra shown in Fig. 5^{21,22}. Malachite cannot be considered a compound added voluntarily to modify the shade of the blue pigment since the green pigment used on these altarpieces was a copper acetate of the type $[\text{Cu}(\text{CH}_3\text{COO})_2]_x[\text{Cu}(\text{OH})_2]_y \cdot n\text{H}_2\text{O}$ incorporating in some cases a basic copper chloride $[\text{CuCl}_2]_x[\text{Cu}(\text{OH})_2]_y \cdot n\text{H}_2\text{O}$. Fig. 6 shows the sequence of painting layers (blue over yellow and ochre layers) from a sample taken from the shawl of the virgin in “The apparition of the Virgin to Saint Francis in the Porciuncula”. The blue paint layer of the shawl (90 μm thick) is formed by coarse azurite particles $2\text{CuCO}_3 \cdot \text{Cu}(\text{OH})_2$ (10 to 20 μm) and a small amount of malachite $\text{CuCO}_3 \cdot \text{Cu}(\text{OH})_2$ detected using $\mu\text{SR-XRD}$ (Fig. 7).

Moreover, mixed with the copper green pigments in green paints, small quantities of azurite were often added to reinforce the blue shade in background landscapes³. Fig. 8 shows a series of infrared spectra from one of the green layers and also an also the corresponding X-ray diffraction pattern.

In order to obtain less saturated blues, the pigment was also dispersed in a white matrix of lead white ($2 \cdot \text{PbCO}_3 \cdot \text{Pb}(\text{OH})_2$ and PbCO_3) and either egg yolk or drying oil binder; therefore, different shades of light blues are obtained by diluting them with a white pigment. Lead carboxylates resulting from the reaction of the free fatty acids from the binder and the lead white are also formed, Fig. 9. Azurite has little tendency to produce Cu carboxylates in contrast to what happens with copper acetates/basic copper acetates and basic copper chlorides used to obtain the green pigments^{1,3}.

Due to the transparency of azurite, the painters frequently prepared lighter or darker blue shades over the ground as a chromatic preparation layer. In the context of 15th century paintings from the Crown of Aragon, the ground layers were composed of gypsum and animal glue. The use of a chromatic preparation layer provided a colour background that highlighted the blue colour of the pigment. In most of the samples, this layer contained a few black carbon particles mixed with lead white, which show a blue shade. Raman microspectroscopy allowed us to determine the presence of these black carbon particles. Fig. 10 shows a series of Raman spectra corresponding to the different layers of a blue painting²¹. The presence of black carbon is detected only in the chromatic preparation layer. Finally, ground azurite or, in other cases, indigo mixed with lead white were also used to obtain a chromatic preparation layer.

As we have shown in Fig. 5 we also found azurite mixed with red and white pigments to obtain violet and also with yellow to obtain purples.

Indigo

Indigo has long been used as a colouring agent. It can be obtained from a great variety of plants whose leaves contain indigo precursors such as indoxyl- β -D-glucoside (indican) and indoxyl-5-ketoglucamate (isatan B). These substances are soluble in water and, through a process of an enzymatic fermentation (β -glucosidase) and later oxidation with atmospheric oxygen, are transformed into a blue substance namely, indigo²³⁻²⁹.

This substance has been used as a dye for fabrics until present, although present-day products are synthetic. Indigo has also been used as a pigment in paintings on illuminated manuscripts, boards, murals and canvas mixed with various binding media.

In the 15th century, in the Western Mediterranean area, indigo could be obtained from the *indigofera tinctoria* L. a plant natural from India traded through Bagdad, Venice and Genova (names that are sometimes associated to the pigment) or from other plants such as *isatis tinctoria* L. (named Pastel in French and woad in English) cultivated in different European areas including some close to the Crown of Aragon, such as Languedoc, between Toulouse and Albi.

The pigment of Asiatic origin was mixed with lime and pressed into small bricks. This material was not cheap but it was quite pure when separated from the lime and dried. However, the product most widely used by painters was that obtained from autochthonous plants which were more accessible, although it was obtained with lower purity.

Indigo in this period was rarely used in the surface layers of the paintings²⁷ and azurite and lapis lazuli were chiefly used. Indigo blue has been identified in the backgrounds of the altarpieces and in the blue painting chromatic preparation layers mixed with lead white.

Indigo can be determined by several analytical methods such as chromatographic techniques, mass spectrometry, surface-enhanced Raman scattering (SERS) that require pre-treatment of the samples. However, its determination is more difficult when appearing in thin inner layers (below 10 μ m) mixed with other materials (lead white, binding media). Fig. 11 shows its identification in a sample taken from the shawl of the virgin in altarpiece by Pascual Ortoneda using μ -FTIR. A good separation is needed to avoid overlapping bands and to obtain an unambiguous determination.

Recent work by Amat et al.²⁹ on spectroscopic properties of indigo dye assigns the infrared experimental bands to the functional groups and those to the theoretical spectrum. In our infrared spectrum from a paint layer a series of bands are identified: 1626 cm^{-1} ν CO, 1614 cm^{-1} shoulder ν CC, 1585 cm^{-1} ν CC δ CH, 1483 cm^{-1} ν CC, 1461 cm^{-1} ν CC, \sim 1400 cm^{-1} δ NH, 1319 cm^{-1} ν CC, 1299 cm^{-1} δ CH, 1196 cm^{-1} ν CC, 1172 cm^{-1} δ CC, 1126 cm^{-1} δ CC, 1077 cm^{-1} ν C-NH-C, (1037 cm^{-1}), (876 cm^{-1}), 754 cm^{-1} δ CH, (748 cm^{-1}), 710 cm^{-1} γ 5-ring, (696 cm^{-1}). We may compare these bands with reference data from the literature^{25,29} and with our own reference spectra of *Isatis Tinctoria* L. (Blue Pastel from Languedoc) and *Indigofera Tinctoria* L. (from Mexico). We observe that the spectra from the *Indigofera Tinctoria* L. dye shows more sharp and clear bands than

that from *Isatis Tinctoria* L. The IR spectrum of the paint compares better to those of *Isatis Tinctoria* L. (Fig. 11d). This could be either a reflection of the low purity of the material, related to the presence of carbohydrates in the raw material. The change in the shape of the spectrum is due to the contribution of the carbonyl and 1200-900 cm⁻¹ carbohydrate absorption bands. Therefore, according to the results obtained, the pigment used in the altarpiece “The Virgin” by Pasqual Ortoneda, the indigo was extracted from nearby plants.

CONCLUSION

This article illustrates how specific sample preparation and a particular combination of analytical techniques can solve most of the problems that may be faced when studying blue paint in altarpieces from the 15th century. To obtain good μ SR-XRD measurements in transmission thin sections, 150 microns thickness, were used. For high angular resolution SR-XRD measurements, small fragments of the sample were placed in a glass capillary to allow spinning which improve the particle statistics. With the aim of obtaining good μ SR-FTIR spectra, measurements in transmission mode were taken using a diamond anvil cell. The results are based in the analyses carried over a number of years on a large sample selection of artworks from the period.

From the study, we may conclude that *lapis lazuli* was used only on very precious artworks. In the case studied it was bound with drying oil and applied only in the most superficial layers of the blue paint. High resolution SR-XRD coupled with the Rietveld method has determined and quantified the minerals constituting the *lapis lazuli* used, which may come from the same source area than those used by Michelangelo. FTIR analysis has shown the presence of absorbed CO₂, which highlights the natural origin of the material. The application of a several layers with a decreasing particle size, first azurite and finishing with *lapis lazuli* relates it to Jan van Eyck’s “Adoration of the Mystic Lamb” with whom shares also clear stylistic resemblances.

Darkening of the azurite painted blue areas is related to the large size of the pigment particles that increase the porosity of the paint where dust from the environment is trapped. This dirt can hardly be removed and is been often consolidated with subsequent varnish layers. Among azurite particles, a few and small BaSO₄ particles, an associated mineral, can also be detected. Due to the weathering of azurite, small quantities of malachite are formed. Aged azurite does not tend to form copper carboxylates in contrast to other copper pigments such as acetates.

Indigo blue was used in large background and chromatic preparation areas. The pigment used in this period and area was principally obtained from plants found in nearby areas (*Isatis Tinctoria* L.).

Reference

- 1 N. Salvadó, S. Butí, M.J. Tobin, E. Pantos, A.J.N.W. Prag, T. Pradell, *Anal. Chem.*, 2005, **77**, 3444-3451.
- 2 N. Salvadó, S. Butí, J. Nicholson, H. Emerich, A. Labrador, T. Pradell, *Talanta*, 2009, **79**, 419-428.
- 3 N. Salvadó, S. Butí, M. Cotte, G. Cinque, T. Pradell, *Appl. Phys. A*, 2013, **111**, 47-57.
- 4 M.T. Domenech-Carbó, *Anal. Chim. Acta*, 2008, **621**, 109-139.
- 5 N. Salvadó, S. Butí, A. Labrador, G. Cinque, H. Emerich, T. Pradell, *Anal. Bioanal. Chem.*, 2011, **399**, 3041-3052.

- 6 N. Salvadó, T. Pradell, E. Pantos, M.Z. Papiz, J. Molera, M. Seco, M. Vendrell-Saz, *J. Synchrotron Radiat.*, 2002, **9**, 215-222.
- 7 D. Creagh, A. Lee, V. Otiero-Alego, M. Kubik, *Radiat. Phys. Chem.*, 2009, **78**, 367-374.
- 8 M. Cotte, P. Dumas, Y. Taniguchi, E. Checroum, P. Walter, J. Susini, *C. R. Physique*, 2009, **10**, 590-600.
- 9 L. Bertrand, L. Robbinet, M. Thoury, K. Janssens, S.X. Cohen, S. Schöder, *Appl. Phys. A*, 2010, **106** (2), 377-396.
- 10 <http://www.mnac.cat>, 2014.
- 11 N. Salvadó, S. Butí, F. Ruiz-Quesada, H. Emerich, T. Pradell, *Butlletí MNAC*, 2008, **9**, 43-61
- 12 P. Coremans, *Studies in Conservation*, 1954, **4**, 145-161.
- 13 J. Plesters in *Artists' Pigments*, ed. Ashok Roy, National Gallery of Art, Washington and Archetype Publications, London 1983, vol. 2 ch. 2, pp. 37-61.
- 14 C. Miliani, A. Daveri, B.G. Brunetti, A. Sgamellotti, *Chem. Phys. Lett.*, 2008, **466**, 148-151
- 15 M. Favaro, A. Guastoni, F. Marini, S. Bianchin, A. Gambirasi, *Anal. Bioanal. Chem.*, 2012, **402**, 2195-2208.
- 16 G.D. Smith, R.J. Klinshaw II, *J. Cult. Herit.*, 2009, **10**, 415-421.
- 17 Cennino Cennini in *Il Libro Dell'Arte*, ed Neri Pozza, Vicenza 1982, pp. 64-69.
- 18 P. Ballirano, A. Maras, *Am. Mineral.*, 2006, **91**, 997-1005.
- 19 M. Clarke, in *Medieval Painters' materials and Techniques, The Montpellier Liber diversarum arcium*, Archetype Publications Ltd. London 2011, 169.
- 20 R.J. Gettens, E. West, in *Artists' Pigments*, ed. Ashok Roy, National Gallery of Art, Washington and Archetype Publications, London 1983, vol. 2 ch. 2, pp. 23-35.
- 21 R.L. Frost, W.N. Martens, L. Rintoul, E. Mahmutagic, J.T. Kloprogge, *J. Raman Spectrosc.*, 2002, **33**, 252-259.
- 22 G.C. Jones, B. Jackson, in *Infrared Transmission Spectra of Carbonate Minerals*, ed. Chapman and Hall, London, 1993.
- 23 H. Schweppe, in *Artists' Pigments*, ed. E. West Fitzhugh, National Gallery of Art, Washington and Archetype Publications, London 1997, vol. 3 ch. 3, pp. 81-98.
- 24 N. Chanayath, S. Lhieochaiphant, S. Phutrakul, *CMU. Journal*, 2002, **1**(2), 149-160.
- 25 A. Baran, A. Fiedler, H. Schulz, M. Baranska, *Anal. Methods*, 2010, **2**, 1372-1376.
- 26 W.S. Laitonjam, S.D. Wangkheirakpam, *Int. J. Plant Physiol. Biochem.*, 2011, **3**(7), 108-116.
- 27 M.H. van Eikema Hommes, Dissertation, UvA, Faculty of Humanities, Amsterdam, 2002, 109-166.
- 28 C. Oberthür, B. Schneider, H. Graf, M. Hamburger, *Chemistry and Biodiversity*, 2004, **1**, 174-182.
- 29 A. Amat, F. Rosi, C. Miliani, A. Sgamellotti, S. Fantacci, *J. Mol. Struct.* 2011, **993**, 43-51.

Acknowledgements

We acknowledge for provision of synchrotron radiation facilities: ESRF under proposals EC-69 (beamline BM01) and CRG 16-01-709/16-01-733 (beamline BM16); ANKA, Germany under proposal EU IA-SFS MS-97 (beamline IR1); Diamond Light Source, UK under proposal EU SM6521 (MIRIAM beamline); and SOLEIL Synchrotron, France under proposal EU 20090887 (beamline SMIS).

N.Salvadó and S. Butí received financial support under MICINN (Spain), grant HAR2009-10790 and under Generalitat de Catalunya, grant 2009SGR01251. T Pradell received financial support under MICINN (Spain), grant MAT2010-20129-C02-01 and under Generalitat de Catalunya, grant 2009SGR01225.

Part of this work was carried out within the framework of agreements of collaboration between the Universitat Politècnica de Catalunya (UPC) and the “Museu Nacional d’Art de Catalunya” (MNAC) and the “Centre de Restauració de Béns Mobles de Catalunya” (CRBMC). We wish to thank the VINSEUM Museum for their collaboration in the study and for the access given to sampling of the altarpiece.

FIGURE CAPTIONS

Figure 1.

- Detail of “Our Lady of the Counsellors” altarpiece by Lluís Dalmau. Dalmau (© MNAC-Museu Nacional d’Art de Catalunya, Barcelona. Photo: Calveras/Mérida/Sagristà)
- Backscattered SEM image from a polished cross section of the blue paint. The red arrow indicates a Ba and S particle.
- μ SR-XRD pattern from (I) the azurite paint layer and (II) the lapis lazuli paint layer

Figure 2.

Observed (crosses) calculated (full line) and difference curve (bottom) data for the Rietveld refinement fit of the high angular resolution synchrotron X-ray powder diffraction pattern of the same sample shown in Figure 1 (*lapis lazuli* paint layer). The bars indicate the position of the Bragg peaks of the different phases.

Figure 3.

μ SR-FTIR spectra corresponding to a) lapis lazuli blue layer (layer II in Figure 1) and b) region where the absorption bands related to CO₂ adsorbed are observed.

Figure 4.

Blue sample from “Constable” altarpiece by Jaume Huguet.

- Bright field OM image from a cross section of the sample.
- Backscattered SEM image from a cross section of the sample. The red arrow indicates a Ba and S particle.

Figure 5.

μ SR-FTIR spectra corresponding to the purple layer of a sample from “The Virgin” altarpiece by Joan Antígó. The purple colour is a mixture of blue, red and white pigments. In the figure, a sequence of spectra related to the compounds identified in the blue pigment is shown.

Figure 6.

- Detail of “The apparition of the Virgin to Saint Francis in the Porciuncula” altarpiece (© MNAC-Museu Nacional d’Art de Catalunya, Barcelona. Photo: Calveras/Mérida/Sagristà)
- Detail of the point where the sample was taken from.
- Polarized light OM image from a polished cross section. The first paint layer corresponds to a yellow surface decoration of the sleeve cuff and contains the lead yellow pigment, -Pb₂SnO₄- and cassiterite -SnO₂-, lead carboxylates, lead oxalates and drying oil (50 μ m thick); the second is an ochre paint layer (30 μ m thick) and contains illite - KAl₂Si₃AlO₁₀(OH)₂-, quartz, colloidal iron hydroxides and drying oil. Below this first two layers, the blue paint layer of the shawl (90 μ m thick) is formed by coarse azurite -2CuCO₃·Cu(OH)₂- particles (10 to 20 μ m), These layers are applied over a gypsum ground layer.

Figure 7.

μ SR-XRD patterns from the sample shown in figure 6, (A) corresponding to layer 1 and (B) corresponding to layers 2/3.

Figure 8.

- Detail of “Our Lady of the Counsellors” altarpiece by Lluís Dalmau (© MNAC-Museu Nacional d’Art de Catalunya, Barcelona. Photo: Calveras/Mérida/Sagristà)
- Polarized light OM image and Backscattered SEM image from a polished cross section of blue/green sample.
- μ SR-XRD pattern of a thin cross section from the blue/green paint layer.

- d) μ SR-FTIR spectra from the blue/green paint layer. I) Azurite $2\text{CuCO}_3\cdot\text{Cu}(\text{OH})_2$, lead white $\text{PbCO}_3/2\text{PbCO}_3\cdot\text{Pb}(\text{OH})_2$ and drying oil, II) azurite $2\text{CuCO}_3\cdot\text{Cu}(\text{OH})_2$ and III) basic copper acetates; drying oil, lead white $\text{PbCO}_3/2\text{PbCO}_3\cdot\text{Pb}(\text{OH})_2$ and oxalates.

Figure 9.

Blue sample from “Saint Vincent” altarpiece by Bernat Martorell

- a) μ SR-FTIR spectra corresponding to the blue layer, I) binding media identified as egg yolk, II) azurite particle and III) lead carboxylates and lead basic carbonate.
b) μ SR-XRD pattern a thin cross section of the blue layer from.

Figure 10.

Blue sample from “Saint John and Saint Stephen” altarpiece by Honorat Borrassà.

- a) Polarized light OM image from a polished cross section of the blue sample.
b) Raman spectra from a polished cross section of the blue sample. From bottom to top: gypsum, lead white, carbon black, iron oxides (goethite), azurite.

Figure 11.

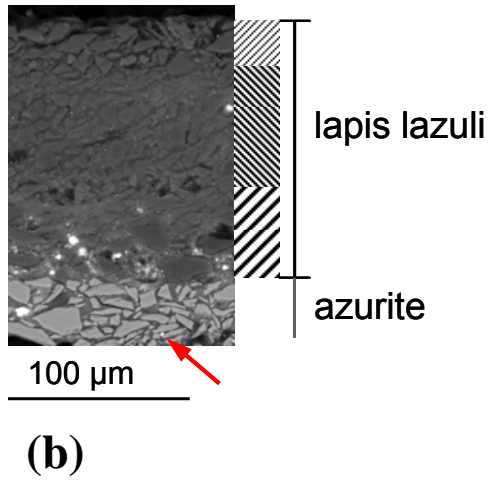
- a) Detail of “The Virgin” altarpiece by Pasqual Ortoneda (© CRBMC- Centre de Restauració de Béns Mobles de Catalunya. Photo: Carles Aymerich)
b) OM image of blue sample. Sequence of layers (from bottom to top): gypsum background, dark blue layer, blue layer and dust/altered superficial layer.
c) μ SR-FTIR spectra corresponding to I) and II) the dark blue layer, III) and IV) blue layer and III) superficial layer.
d) $2000\text{-}650\text{cm}^{-1}$ region of μ SR-FTIR spectrum II of figure 11c. Indigo from paint layer (spectrum III) is compared to indigo from *Isatis Tintorea* L. (spectrum II) and indigo from *Indigofera Tintorea* L. (spectrum I).

Table 1.

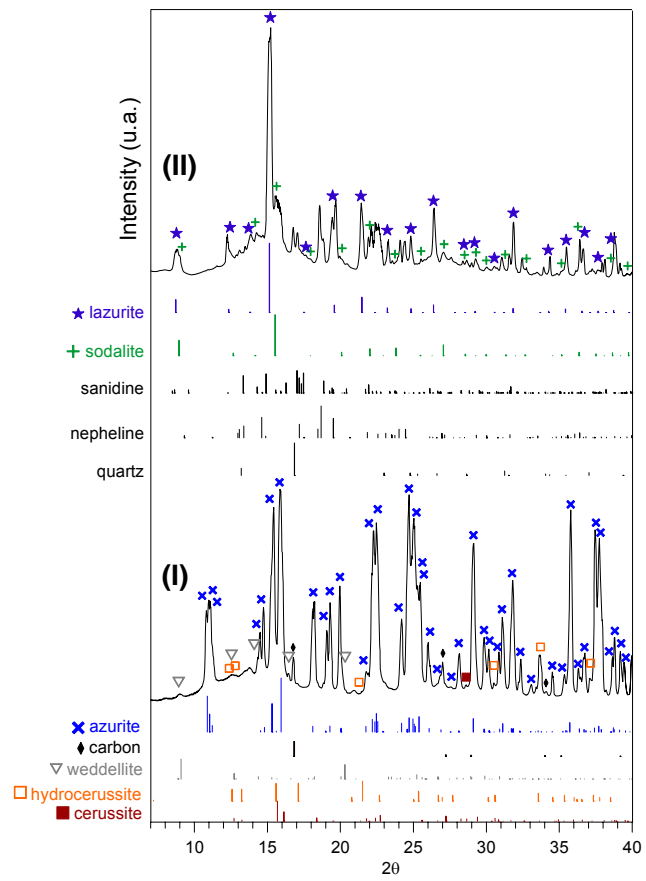
Rietveld quantitative phase analysis results (phase contents and unit cell data) for a *lapis lazuli* sample of “The Virgin of the Counsellors” by Lluís Dalmau.

Table 1. Rietveld quantitative phase analysis results (phase contents and unit cell data) for a *lapis lazuli* sample of “The Virgin of the Counsellors” by Lluís Dalmau.

	wt%	phase	wt%	a/Å	b/Å	c/Å	α°	β°	γ°	V/Å ³
lapis lazuli layer 75.4%	62.5	lazurite	47.1(2)	9.0800(2)	9.0800(1)	9.0800(2)	90	90	90	748.61(4)
	23.6	nepheline	17.8(1)	10.0001(3)	10.0001(3)	10.0001(3)	90	90	120	726.22(4)
	6.9	quartz	5.2(1)	4.9114(3)	4.9114(3)	5.4033(6)	90	90	120	112.88(1)
	6.1	sodalite	4.6(2)	8.8712(7)	8.8712(7)	8.8712(7)	90	90	90	698.1(2)
	1.0	sanidine	0.8(2)	8.552(5)	12.997(6)	7.188(3)	90	115.99	90	718.1(4)
Azurite-layer 24.6%		azurite	24.6(1)	5.0071(1)	5.8440(1)	10.3420(2)	90	92.42	90	302.35(1)



(a)



(c)

Figure 1

Lapis lazuli _ sample D3 _ BM01B
Lambda 0.3749 A, L-S cycle 897

Hist 1
Obsd. and Diff. Profiles

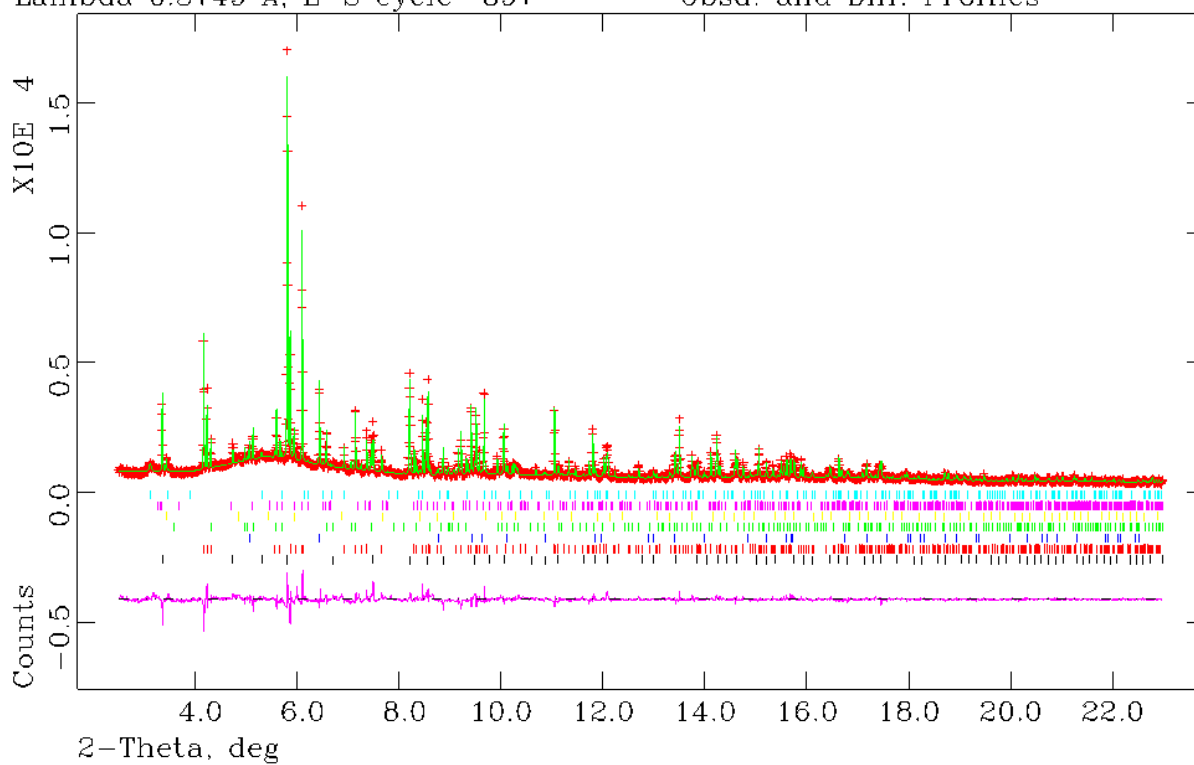
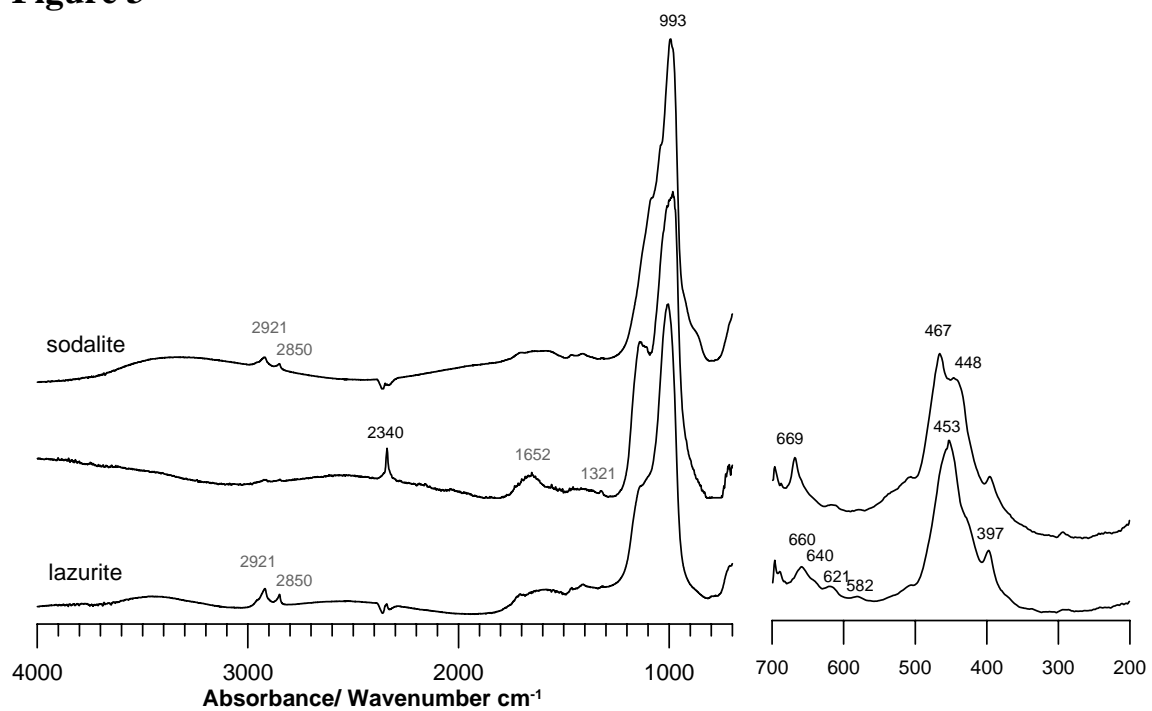
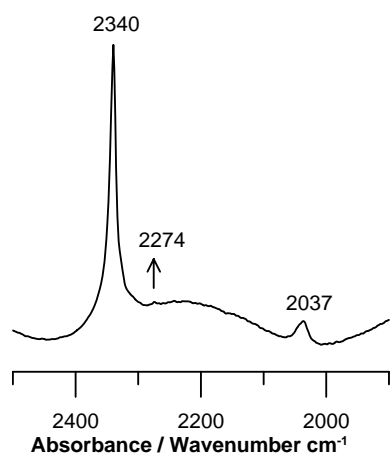


Figure 2

Figure 3

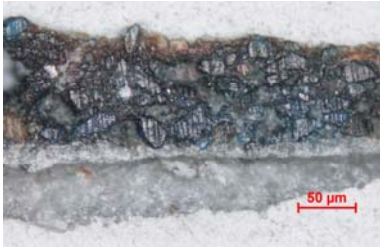


(a)

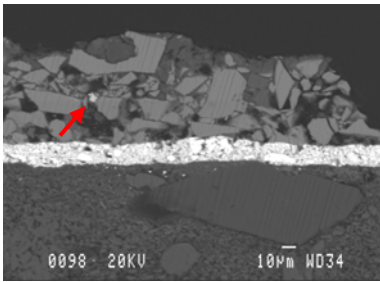


(b)

Figure 4



(a)



(b)

Figure 5

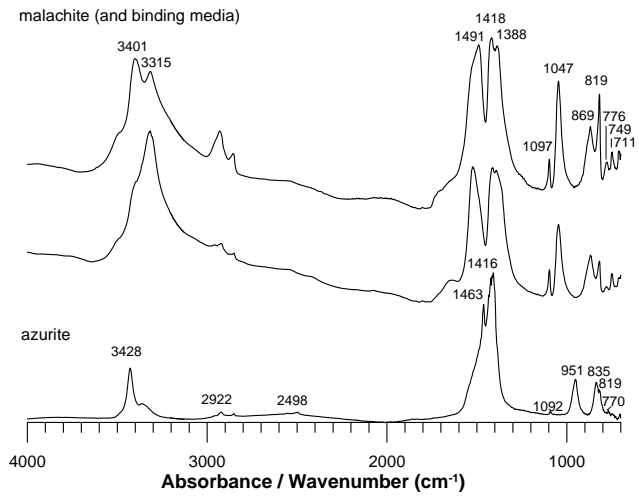


Figure 6.

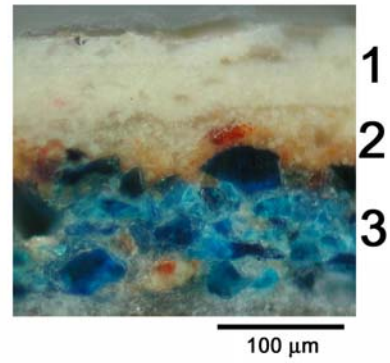


Figure 7.

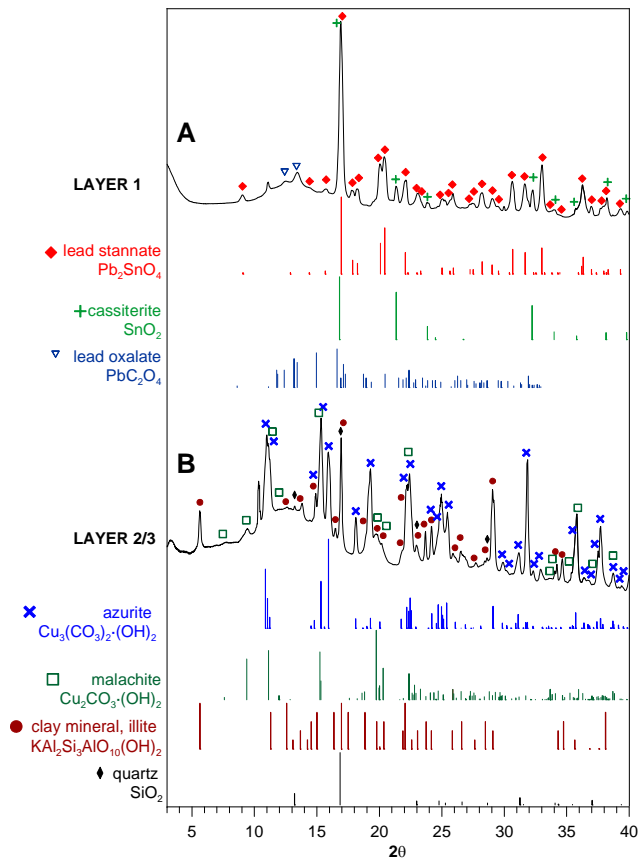
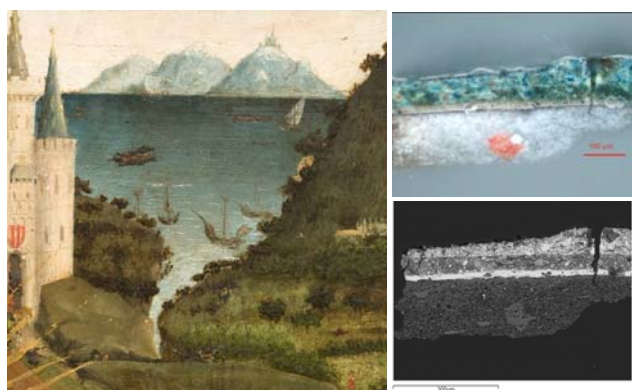
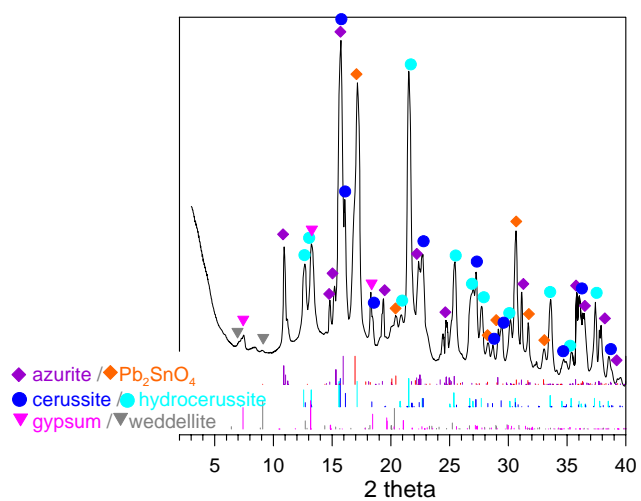


Figure 8.

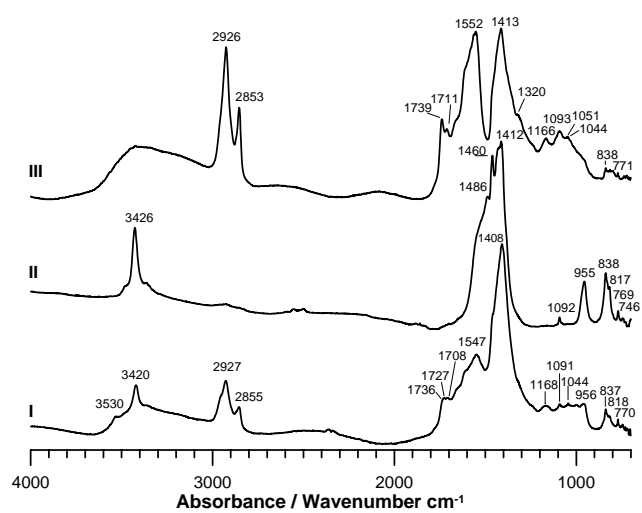


(a)

(b)

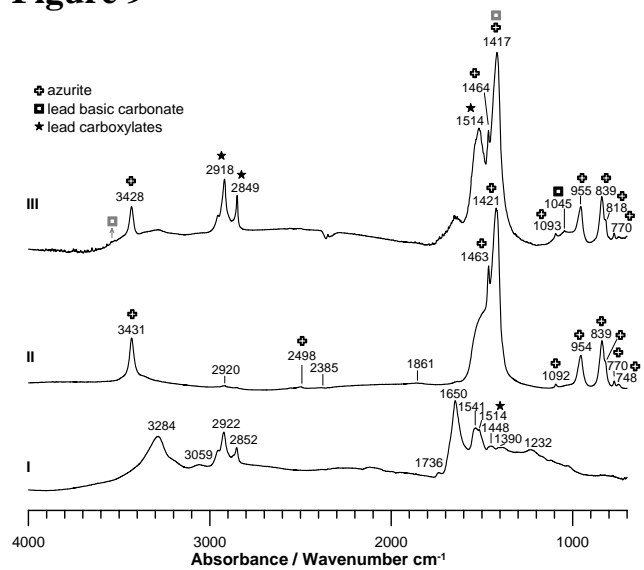


(c)

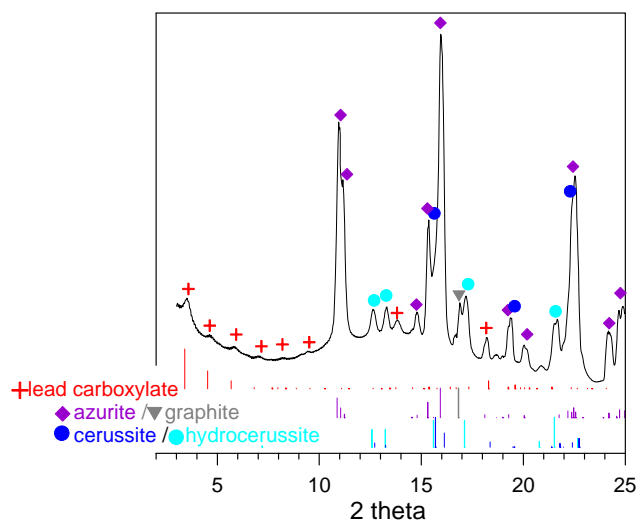


(d)

Figure 9

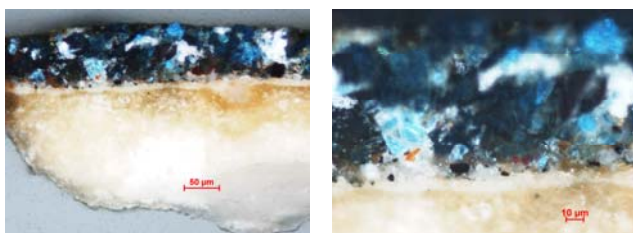


(a)

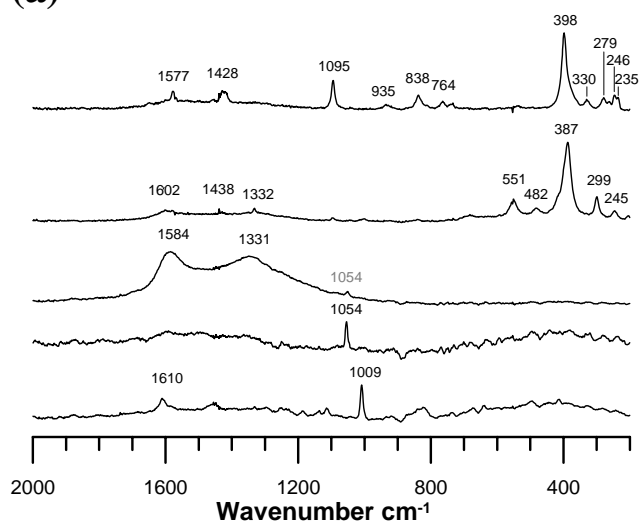


(b)

Figure 10



(a)



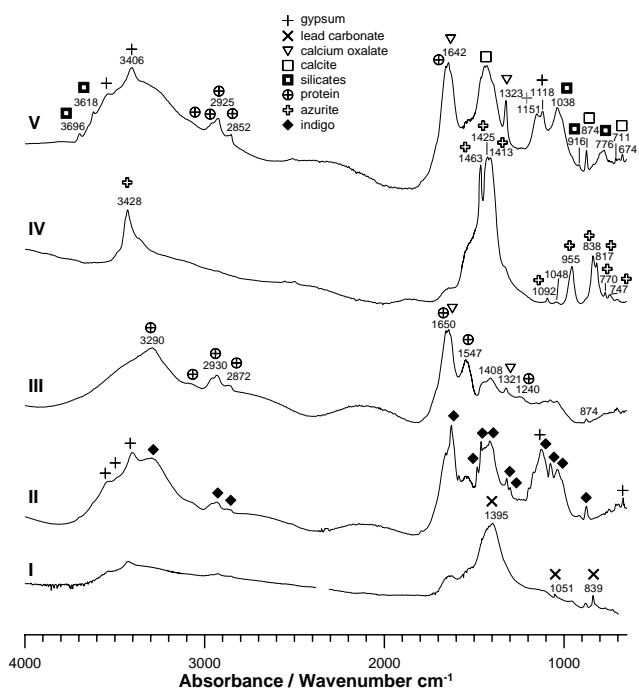
(b)

Figure 11.

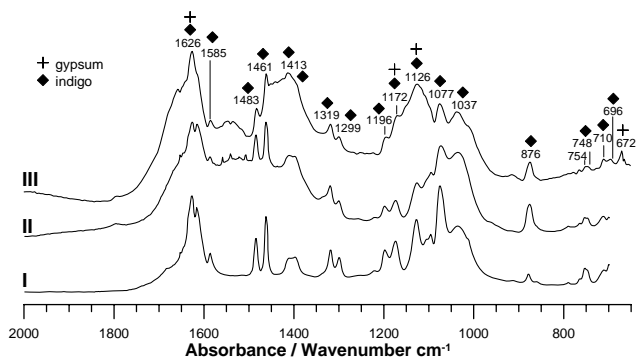


(a)

(b)



(c)



(d)